


UCRL-JC-127963
PREPRINT

Low Amplitude Impact Testing and Analysis of Pristine and Aged Solid High Explosives

Steven K. Chidester
Craig M. Tarver
Raul Garza

This paper was prepared for submittal to the
Eleventh International Detonation (1998) Symposium
Snowmass, CO
Aug: 31- Sept. 4, 1998

August 17, 1998



Lawrence
Livermore
National
Laboratory

This is a preprint of a paper intended for publication in a journal or proceedings. Since changes may be made before publication, this preprint is made available with the understanding that it will not be cited or reproduced without the permission of the author.

DISCLAIMER

This document was prepared as an account of work sponsored by an agency of the United States Government. Neither the United States Government nor the University of California nor any of their employees, makes any warranty, express or implied, or assumes any legal liability or responsibility for the accuracy, completeness, or usefulness of any information, apparatus, product, or process disclosed, or represents that its use would not infringe privately owned rights. Reference herein to any specific commercial product, process, or service by trade name, trademark, manufacturer, or otherwise, does not necessarily constitute or imply its endorsement, recommendation, or favoring by the United States Government or the University of California. The views and opinions of authors expressed herein do not necessarily state or reflect those of the United States Government or the University of California, and shall not be used for advertising or product endorsement purposes.

LOW AMPLITUDE IMPACT TESTING AND ANALYSIS OF PRISTINE AND AGED SOLID HIGH EXPLOSIVES

Steven K. Chidester, Craig M. Tarver, and Raul Garza
Lawrence Livermore National Laboratory
Livermore, CA 94551

The critical impact velocities of 60.1 mm diameter blunt steel projectiles required for ignition of exothermic chemical reaction were determined for heavily confined charges of new and aged (15-30 years) solid HMX-based high explosives. The explosives in order of decreasing impact sensitivity were: PBX 9404; LX-10; LX-14; PBX 9501; and LX-04. Embedded pressure gauges measured the interior pressure histories. Stockpile aged LX-04 and PBX 9501 from dismantled units were tested and compared to freshly pressed charges. The understanding of explosive aging on impact ignition and other hazards must improve as systems are being deployed longer than their initial estimated lifetimes. The charges that did not react on the first impact were subjected to multiple impacts. While the violence of reaction increased with impact velocity, it remained much lower than that produced by an intentional detonation. Ignition and Growth reactive flow models were developed to predict HMX-based explosive impact sensitivity in other geometries and scenarios.

INTRODUCTION

Impact sensitivity of solid high explosives is an important concern in handling, storage, and shipping procedures. Several impact tests have been developed for specific accident scenarios, but these tests are generally neither reproducible nor amenable to computer modeling. The Steven impact test¹ was developed with these objectives in mind. Critical impact velocities for exothermic chemical reaction were determined for new and aged charges of five HMX-based explosives: LX-10-1 (94.5wt% HMX, 5.5wt% Viton A binder); LX-04 (85wt% HMX, 15wt% Viton A); PBX 9404 (94wt% HMX, 3wt% nitrocellulose, 3wt% CEF binder); LX-14 (95.5wt% HMX, 4.5wt% Estane binder); and PBX 9501 (94.9wt% HMX, 2.5wt% BDNPA-F, 2.5wt% Estane binder, 0.1wt% DPA or Irganox). Blast wave overpressure gauges, external strain gauges and embedded pressure gauges were used to measure the relative violence of the explosive reactions. The blast wave overpressures produced by intentional detonations of several different explosive charges were measured for comparison. The Ignition and Growth reactive flow model tested several impact ignition criteria and simulated the growth of

explosive reaction following ignition as the confined explosive charge is producing gaseous reaction products. Empirical reaction rate models for the five explosives were developed for impact sensitivity estimations.

EXPERIMENTAL GEOMETRY

The experimental geometry for the Steven impact test is shown in Fig. 1. A 6.01 cm diameter steel projectile is accelerated by a gas gun into 11 cm diameter by 1.285 cm thick explosive charges confined by 0.3175 cm thick steel plates on the impact face and 1.905 cm thick steel plates on the back side. The original Steven test used a 6.01 cm diameter tantalum rod or rounded projectile.¹ DYNA2D calculations showed that the high explosive was driven to violent explosions by the frictional work done in the region where the tantalum projectile struck.¹ Since the objective of this study was to determine thresholds for low order reactions and to measure relative reaction violence of these explosions, the projectiles were changed to steel to provide less frictional work on the explosive and to allow the 76.2 mm diameter gas gun to

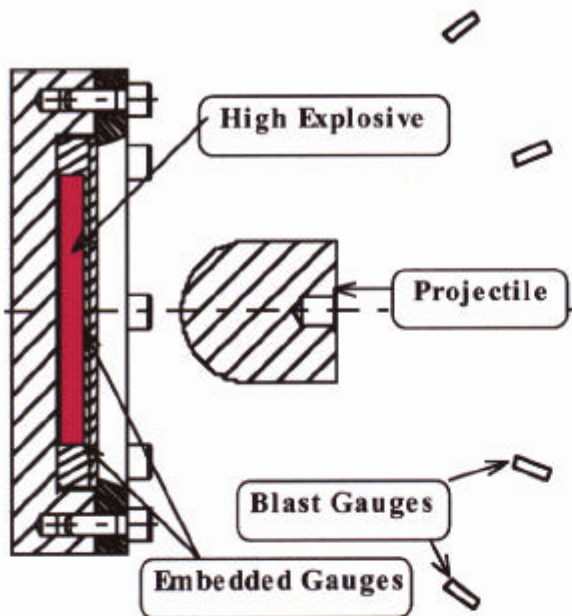


FIGURE 1. GEOMETRY OF THE STEVEN IMPACT TEST

accelerate these projectiles to the higher velocities required to ignite LX-04. Four external blast overpressure gauges were placed ten feet from each target for direct comparison with Susan test data.² As shown in Fig. 1, in two locations there are embedded pressure gauges which are being used to measure the internal pressure developed during the impact and the subsequent growth of reaction if the critical impact velocity is exceeded. Figure 2 shows the exact locations of the two types of gauges: four carbon resistance gauges located between the Teflon retaining ring and explosive sample and two carbon foil gauges located between the cover plate and the explosive sample.

EXPERIMENTAL RESULTS

Intentional detonations were performed for direct comparison to the reactions from projectile impact. Table 1 presents the four intentional detonations of various amounts of explosives. The explosives used for the intentional detonations were comprised of TNT with some Composition B. Two intentional detonations were performed with identical 120 gram explosive charges, and the resulting measured average

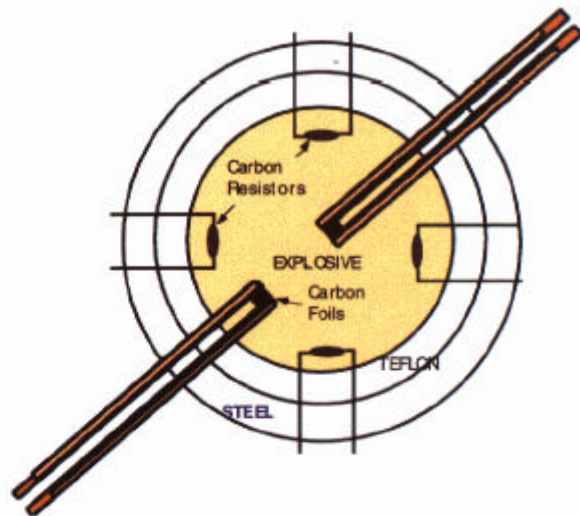


FIGURE 2. PLACEMENT OF THE CARBON RESISTOR AND CARBON FOIL GAUGES IN THE EXPLOSIVE TARGET

overpressures were virtually identical. This type of repeated test provides confidence that the overpressure gauges are working correctly.

The results of 45 Steven tests are listed in Table 2. The type of explosive, the density of the charge, the projectile velocity, whether reaction was observed or not, and the average overpressure measured in pounds per square inch by the four blast gauges are included in Table 2. The critical impact velocities for the five HMX-based explosives are in the usual order of decreasing impact sensitivity: PBX 9404; LX-10-1; LX-14; PBX 9501; and LX-04. In contrast to other impact tests, such as the Susan and Skid tests,² the Steven test yields a true cut-off critical velocity with no reactions observed at lower velocities. With the possible exception of PBX 9404, the Steven test also yields relatively low order reactions which can be quantitatively measured by blast overpressure gauges and related to an equivalent amount of TNT. Figure 3 shows the average overpressures measured by the blast wave gauges for the four explosives as functions of projectile impact velocity. In this figure, the term virgin refers to an explosive charge that was never in the stockpile. For example, the virgin (new or pristine) PBX 9501 (HOL89C730-010) was formulated in 1989 and pressed in 1997. The use of steel projectiles allows low order reactions to be observed in LX-10, whereas

TABLE 1. SUMMARY OF INTENTIONAL DETONATION EXPERIMENTS

Explosive	Density (g/cm ³)	mass (g)	Average Overpressure (psi)
TNT	1.635	175	14.30
TNT	1.635	345	18.03
TNT	1.635	120	11.86
TNT	1.635	120	11.93

the tantalum projectiles used by Chidester, et al.¹ produced only violent explosions in LX-10. The abrupt increases in overpressure measured for PBX 9404 and LX-10-1 and the much slower increases measured for PBX 9501 and LX-04 are similar to those obtained in the Susan test. Steven test results compared closely to Susan test results in terms of the TNT equivalent weight that would produce the same average overpressures at a distance of ten feet. Even though the Steven test uses approximately one half as much explosive as the Susan test, it produces larger overpressures at the same projectile impact velocity. This is due to the greater confinement in the Steven test, which uses two steel plates, compared to the thin aluminum cap that confines the explosive charge in the Susan test. This increased confinement allows the chemical reaction to grow further and produce more gas before the steel confinement (0.3175 cm cover plate) of the Steven test is breached, and the subsequent rarefaction waves slow the reaction to a deflagration-type process.

The unreacted targets were subjected to multiple impacts until a explosive reaction was obtained. Table 3 presents the results of the multiple impact tests that have been performed thus far, namely PBX 9404 and LX-10. The other unreacted targets have been scheduled but not completed in time for this publication. The threshold impact velocity necessary to cause a reaction in a previously damaged target is typically less than that of a pristine or undamaged assembly. The amount of reduction is in the range of 9 to 11% of the velocity necessary for an undamaged explosive reaction, which is less than previous work¹ where the reduction seen with LX-10 was 33%. One of our recent projectile impacts on previously damaged PBX 9404 resulted in 12.6 psi overpressure, which is slightly more (see Table 1)

than the overpressure from a 120 gram TNT detonation. However, since the Steven test uses 224 grams of PBX 9404 and HMX contains more energy per gram than TNT, this high overpressure from PBX 9404 does not represent complete reaction of the charge. Reactions from other multiple hits on HMX-based explosives resulted in much lower overpressures similar to those presented in previous work¹ and those presented in Table 2 for single impact tests. The two PBX 9404 reactions occurring nearly at identical velocities give evidence that the threshold velocity is independent of the quantity of prior damage. These kinds of test results are necessary to be able to make assessments of explosive assembly safety following an accident.

Table 4 shows the tested threshold impact velocities for various HMX-based explosives. The LX-14 data consists of two ages (0 and 96 months), but, since the aging did not occur in the stockpile, the stockpile age is denoted with an asterisk in the age column. Although concise thresholds for the two LX-14 sample sets were obtained and showed no significant impact threshold difference, additional testing is planned to understand the relationship between increasing impact velocity and violence of reaction, such as is presented in Fig. 3. As expected, PBX 9404 was found to have the lowest impact threshold velocity. The experimental uncertainty is shown in parentheses under the threshold velocity value. The threshold velocity value is defined as the lowest impact velocity for which the explosive reacted thus far. To better determine this threshold and reduce the experimental uncertainty, additional testing is required between the lowest velocity for observed reaction and the highest velocity for which there was no reaction from the projectile impact. Further testing is planned to narrow in on the threshold impact velocity and reduce the experimental uncertainty for several of these explosives. At this point in the testing, it is too early to draw definite conclusions about differences in impact sensitivity due to explosive aging. Enough testing has been accomplished to support the statement that there has not been any drastic reduction in threshold impact velocity due to explosive aging.

TABLE 2. SUMMARY OF THE STEVEN SINGLE IMPACT TEST EXPERIMENTS

Explosive	Density (g/cm ³)	Projectile Velocity (m/s)	Reaction	Average Overpressure (psi)
PBX 9404	1.835	23.00	No	N.A.
PBX 9404	1.835	31.00	No	N.A.
PBX 9404	1.835	34.00	Yes	3.200
PBX 9404	1.835	39.00	Yes	10.000
LX-10-1	1.865	35.00	No	N.A.
LX-10-1	1.865	41.50	Yes	N.R.
LX-10-1	1.865	46.50	Yes	6.400
LX-10-1	1.865	47.00	Yes	5.800
LX-14	1.822	39.30	No	N.A.
LX-14	1.823	41.20	Yes	1.325
LX-14	1.821	46.30	Yes	1.625
LX-14 (aged)	1.823	40.00	No	N.A.
LX-14 (aged)	1.823	41.48	Yes	1.875
LX-14 (aged)	1.823	44.80	Yes	2.550
PBX 9501	1.843	34.00	No	N.A.
PBX 9501	1.843	39.00	No	N.A.
PBX 9501	1.843	43.00	Yes	1.900
PBX 9501	1.843	53.00	Yes	2.050
PBX 9501	1.843	56.00	Yes	2.500
PBX 9501	1.843	63.00	Yes	3.930
PBX 9501	1.843	66.50	Yes	3.675
PBX 9501	1.843	68.00	Yes	N.R.
PBX 9501	1.829	38.00	No	N.A.
PBX 9501	1.830	43.00	No	N.A.
PBX 9501	1.829	53.40	Yes	1.550
PBX 9501	1.829	59.07	Yes	2.525
PBX 9501	1.829	61.06	Yes	2.250
PBX 9501 (aged)	1.830	40.00	No	N.A.
PBX 9501 (aged)	1.830	43.36	Yes	1.100
PBX 9501 (aged)	1.830	55.41	Yes	3.600
PBX 9501 (aged)	1.830	59.14	Yes	2.150
PBX 9501 (aged)	1.830	66.58	Yes	4.020
LX-04	1.870	40.00	No	N.A.
LX-04	1.870	45.00	Yes	0.200
LX-04	1.870	81.00	Yes	1.825
LX-04	1.871	90.00	Yes	2.525
LX-04	1.870	98.00	Yes	2.300
LX-04	1.870	110.00	Yes	2.925
LX-04 (aged)	1.868	37.00	No	N.A.
LX-04 (aged)	1.861	40.00	No	N.A.
LX-04 (aged)	1.862	43.00	Yes	0.400
LX-04 (aged)	1.862	45.50	Yes	0.325
LX-04 (aged)	1.867	50.80	Yes	1.020
LX-04 (aged)	1.866	90.60	Yes	2.310
LX-04 (aged)	1.868	98.16	Yes	2.806

TABLE 3. SUMMARY OF THE STEVEN MULTIPLE IMPACT EXPERIMENTS

Explosive	Density (g/cm ³)	Projectile Impact #	Projectile Velocity (m/s)	Average Overpressure (psi)
PBX 9404	1.835	2	27.52	None
PBX 9404	1.835	3	28.99	None
PBX 9404	1.835	4	30.03	None
PBX 9404	1.835	5	30.99	12.60
PBX 9404	1.835	4	27.36	None
PBX 9404	1.835	5	31.09	3.20
LX-10-1	1.865	2	29.62	None
LX-10-1	1.865	3	32.70	None
LX-10-1	1.865	4	34.05	None
LX-10-1	1.865	5	36.22	None
LX-10-1	1.865	6	36.80	4.03

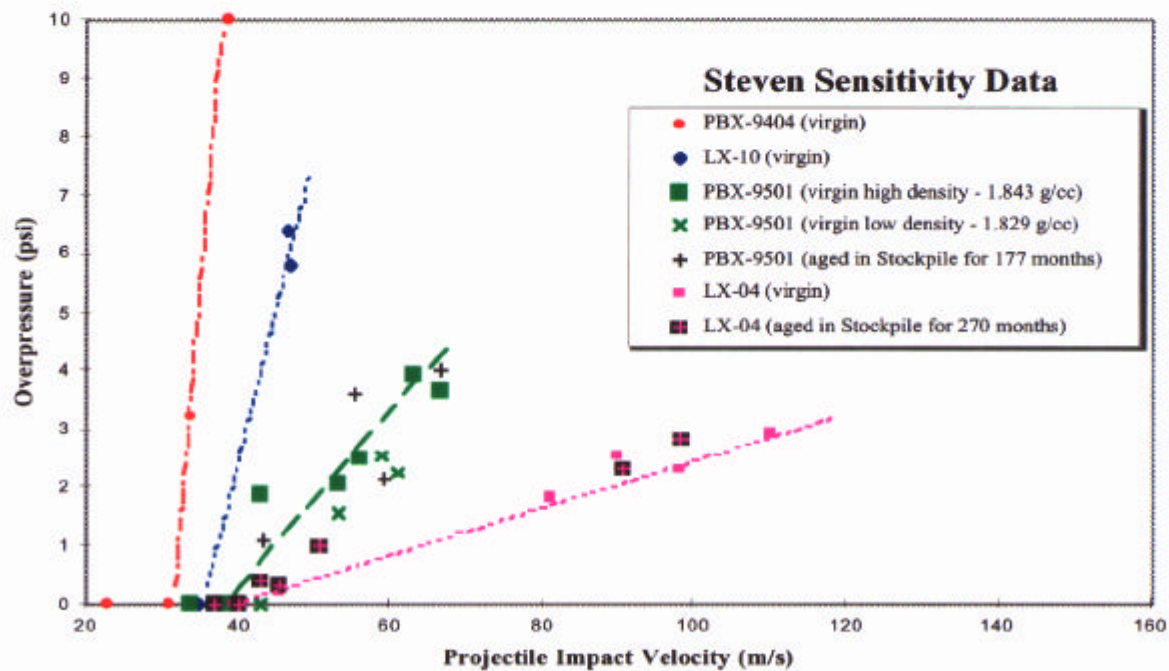


FIGURE 3. BLAST OVERPRESSURES VERSUS PROJECTILE IMPACT VELOCITY

TABLE 4. SUMMARY OF EXPLOSIVE EXPERIMENTAL THRESHOLDS

Explosive	Density (g/cm ³)	Stockpile Age (months)	Threshold Velocity (m/s)
PBX 9404	1.835	0	34.0 (+0, -3.0)
PBX 9404 Damaged	1.835	0	30.9 (+0, -0.9)
LX-10	1.865	0	41.5 (+0, -6.5)
LX-10 Damaged	1.865	0	36.8 (+0, -0.6)
LX-14	1.822	0	41.2 (+0, -1.9)
LX-14	1.823	96 *	41.5 (+0, -1.5)
LX-04	1.870	0	45.0 (+0, -5.0)
LX-04	1.865	270	43.0 (+0, -3.0)
PBX 9501	1.843	0	43.0 (+0, -4.0)
PBX 9501	1.829	0	53.4 (+0, -10.3)
PBX 9501	1.830	177	43.4 (+0, -3.3)

IGNITION AND GROWTH REACTIVE FLOW MODEL

The first DYNA2D modeling of the Steven test¹ concentrated on its mechanical aspects. The measured depths of dents in the targets that did not react were accurately calculated, and a constant frictional work criteria for LX-10-1 was developed. Chidester et al.³ then modified the Ignition and Growth reactive flow model developed for shock initiation and detonation to calculate reaction rates under impact ignition conditions. The Ignition and Growth reactive flow model uses two Jones-Wilkins-Lee (JWL) equations of state, one for the unreacted explosive and one for the reaction products:

$$p = A e^{-R_1 V} + B e^{-R_2 V} + \omega C_V T/V \quad (1)$$

where p is the pressure in Megabars, V is the relative

volume, T is temperature, ω is the Gruneisen coefficient, C_V is the average heat capacity, and A, B, R_1 and R_2 are constants. The reaction rate law is:

$$\begin{aligned} dF/dt = & I(1-F)^b(\rho/\rho_0-1-a)^x + G_1(1-F)^c F^d p^y \\ & 0 < F < F_{igmax} \quad 0 < F < F_{G1max} \\ & + G_2(1-F)^e F^g p^z \\ & F_{G2min} < F < 1 \end{aligned} \quad (2)$$

where F is the fraction reacted, t is time in μs , ρ is the current density in g/cm³, ρ_0 is the initial density, p is pressure in Mbars, and I, G_1 , G_2 , a, b, c, d, e, g, x, y, and z are constants. This three term reaction rate law models the three stages of reaction observed during impact or shock initiation of pressed solid explosives.⁴ For these low pressure (0.1 GPa), long time (several hundred μs) impacts, the first term in Eq. (2) uses $x = 4$ to simulate a constant input energy ignition criterion, which works for PBX 9404 at both low and high pressures. The equations of state and growth of reaction rates are the standard ones for LX-10-1 shock initiation.⁴ Using $I=1000 \mu s^{-1}$ in Eq. (2) yields an ignition rate similar to that predicted by the 0.37 cal/cm² frictional work criterion for LX-10-1 ignition used by Chidester et al.¹ Table 5 lists the parameters used to calculate the measured critical impact velocities for the five HMX-based explosives, and Table 6 lists the Gruneisen equation of state parameters used for the inert materials.

Figure 4 shows the pressure histories for several LX-10-1 elements directly under the steel projectile for an impact velocity of 39 m/s. The maximum impact pressure is 0.1 GPa and lasts about 80 μs . Rapid reaction occurs about 335 μs after impact and at a fraction reacted of about 0.15%. Also shown in Fig. 4 are the embedded pressure gauge records for this experiment. The carbon foil gauge located in the impact region measured a peak pressure and time duration very similar to the calculated values. Four carbon resistor gauges located near the outside of the explosive charge and the Teflon confining ring, along with framing camera data, detected exothermic reaction 360 μs after impact, in excellent agreement with the calculated time of 335 μs . Therefore this Ignition and Growth model predicts quite well the measured impact pressure and pulse duration and the subsequent time to exothermic reaction and is being used to estimate relative impact sensitivity.

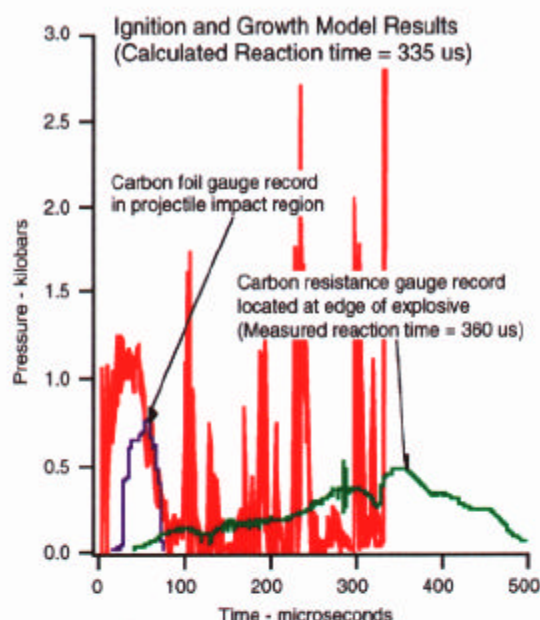


FIGURE 4. COMPARISON OF EMBEDDED PRESSURE GAUGE MEASUREMENTS AND REACTIVE FLOW CALCULATIONS

SUMMARY AND CONCLUSIONS

The understanding of material aging must improve when weapons and other systems are being deployed longer than their initial estimated lives. Testing and analysis that is presented here and by others^{5,6} needs to be continued to gain the required knowledge. Analysis of the testing helps to determine the reaction mechanisms and provides tools to accurately predict the response of an accident scenario. Since all accident scenarios can not be tested in a useful time, reliable models based on data from well-instrumented and reproducible experiments are necessary. However, to develop predictive reactive flow models that can reliably simulate a wide variety of impact scenarios, a great deal of experimental and theoretical work must be done on the fundamental physical and chemical processes which determine the ignition rates of that first small amount of explosive that starts the exothermic process. The various postulated processes that may heat the explosive to thermal decomposition, such as friction, shear, void collapse, etc., have to be isolated and quantitatively measured in well diagnosed experiments. Then it must be determined experimentally and theoretically which process is

responsible for ignition under each set of conditions produced by various impact scenarios. Only then can reliable predictions of the impact safety and useful lifetimes of high explosives be made.

ACKNOWLEDGMENTS

The authors would like to thank Jerry Forbes and Frank Garcia for obtaining the embedded pressure gauge records and Cynthia Nitta, Roger Logan, LeRoy Green, and Anthony DePiero for their support. This work was performed under the auspices of the U.S. Department of Energy by Lawrence Livermore National Laboratory (contract no. W-7405-ENG-48).

REFERENCES

1. Chidester, S. K., Green, L. G., and Lee, C. G., Tenth International Detonation Symposium, Office of Naval research 33395-12, Boston, MA, 1993, p. 785.
2. Dobratz, B. M. and Crawford, P. C., LLNL Explosives Handbook, Lawrence Livermore National Laboratory Report UCRL-52997 Change 2, 1985.
3. Chidester, S. K., Tarver, C. M. Tarver, and Lee, C. G., Shock Compression of Condensed Matter-1997, S. C. Schmidt, D. P. Dandekar, and J. W. Forbes, eds., AIP Conference Proceedings 429, New York, 1998, p. 707.
4. Tarver, C. M., Urtiew, P. A., Chidester, S. K., and Green, L. G., Propellants, Explosives, Pyrotechnics **18**, 117 (1993).
5. Browning, R. V., Shock Compression of Condensed Matter-1995, S. C. Schmidt and W. C. Tao, eds., AIP Press, New York, 1996, p. 405.
6. Idar, D. J., Lucht, R. A., Scammon, R., Straight, J., and Skidmore, C. B., "PBX 9501 High Explosive Violent Response/ Low Amplitude Insult Project," Los Alamos National Laboratory Report LA-13164-MS, UC-741, 1997.

TABLE 5. REACTIVE FLOW PARAMETERS FOR IMPACT IGNITION

A. LX-10		$\rho_0 = 1.865 \text{ g/cm}^3$	
UNREACTED JWEL EOS	PRODUCT JWEL EOS	REACTION RATES	
A=9522 Mbar	A=8.807 Mbar	$I=1000 \mu\text{s}^{-1}$	
B=-0.05944 Mbar	B=0.1836 Mbar	$a=0$	
$R_1=14.1$	$R_1=4.62$	$b=0.667$	
$R_2=1.41$	$R_2=1.32$	$x=4.0$	$F_{igmax}=0.3$
$w=0.8867$	$w=0.38$	$G_1=120 \text{ Mbar}^{-2} \mu\text{s}^{-1}$	
$C_V=2.7806 \times 10^{-5} \text{ Mbar/K}$	$C_V=1.0 \times 10^{-5} \text{ Mbar/K}$	$c=0.667$	$d=0.333$
$T_0=298^\circ\text{K}$	$E_0=0.104 \text{ Mbar}$	$y=2.0$	$FG1_{max}=0.5$
Shear Modulus=0.050 Mbar		$G_2=400 \text{ Mbar}^{-3} \mu\text{s}^{-1}$	
Yield Strength=0.0003 Mbar		$e=0.333$	$g=1.0$
		$z=3.0$	$FG2_{min}=0.5$
Calculated Critical impact velocity = 38 - 39 m/s		Calculated time to reaction = 338 μs	
B. PBX 9404		$\rho_0 = 1.835 \text{ g/cm}^3$	$G_1 = 160 \text{ Mbar}^{-2} \mu\text{s}^{-1}$
Calculated Critical impact velocity = 33 - 34 m/s		Calculated time to reaction = 438 μs	
C. PBX 9501		$\rho_0 = 1.843 \text{ g/cm}^3$	$G_1 = 118 \text{ Mbar}^{-2} \mu\text{s}^{-1}$
Calculated Critical impact velocity = 42 - 43 m/s		Calculated time to reaction = 190 μs	
D. LX-04		$\rho_0 = 1.865 \text{ g/cm}^3$	$G_1 = 115 \text{ Mbar}^{-2} \mu\text{s}^{-1}$
Calculated Critical impact velocity = 43 - 44 m/s		Calculated time to reaction = 253 μs	
E. LX-14		$\rho_0 = 1.823 \text{ g/cm}^3$	$G_1 = 119 \text{ Mbar}^{-2} \mu\text{s}^{-1}$
Calculated Critical impact velocity = 41 - 42 m/s		Calculated time to reaction = 260 μs	

TABLE 6. GRUNEISEN EOS PARAMETERS FOR INERT MATERIALS

$p = \rho_0 c^2 \mu [1 + (1 - \gamma_0/2)\mu - a/2\mu^2] / [1 - (S_1 - 1)\mu - S_2\mu^2/(\mu + 1) - S_3\mu^3/(\mu + 1)^2]^2 + (\gamma_0 + a\mu)E,$ <p style="text-align: center;">where $\mu = \rho/\rho_0 - 1$ and E is thermal energy</p>							
INERT	$\rho_0(\text{g/cm}^3)$	$c(\text{mm}/\mu\text{s})$	S_1	S_2	S_3	γ_0	a
Al 6061	2.703	5.24	1.4	0.0	0.0	1.97	0.48
Steel	7.90	4.57	1.49	0.0	0.0	1.93	0.5
Teflon	2.15	1.68	1.123	3.98	-5.8	0.59	0.0